

Retention of gene products in syncytial spermatids promotes non-Mendelian inheritance as revealed by the *t complex responder*

Nathalie Véron,^{1,2} Hermann Bauer,¹
 Andrea Y. Weiße,^{3,6} Gerhild Lüder,⁴
 Martin Werber,^{1,5} and Bernhard G. Herrmann^{1,5,7}

¹Department of Developmental Genetics, Max-Planck-Institute for Molecular Genetics, 14195 Berlin, Germany; ²Faculty of Biology, Free University Berlin, 14195 Berlin, Germany;

³Department of Mathematics and Computer Science, Biocomputing Group, Free University Berlin, 14195 Berlin, Germany; ⁴Electron Microscopy Group, Max-Planck-Institute for molecular Genetics, 14195 Berlin, Germany; ⁵Institute for medical Genetics-CBF, Charité-University Medicine Berlin, 12203 Berlin, Germany

The *t complex responder* (*Tcr*) encoded by the mouse *t* haplotype is able to cause phenotypic differences between *t* and + sperm derived from *t/+* males, leading to non-Mendelian inheritance. This capability of *Tcr* contradicts the concept of phenotypic equivalence proposed for sperm cells, which develop in a syncytium and actively share gene products. By analyzing a *Tcr* minigene in hemizygous transgenic mice, we show that *Tcr* gene products are post-meiotically expressed and are retained in the haploid sperm cells. The wild-type allele of *Tcr*, *sperm motility kinase-1* (*Smok1*), behaves in the same manner, suggesting that *Tcr/Smok* reveal a common mechanism prone to evolve non-Mendelian inheritance in mammals.

Supplemental material is available at <http://www.genesdev.org>.

Received August 14, 2009; revised version accepted October 12, 2009.

Diploid organisms transmit homologous chromosomes at an equal (the Mendelian) ratio to their offspring. However, several exceptions have been observed all across the animal kingdom and have puzzled geneticists for decades (Hurst and Werren 2001). In mammals, the mouse *t* haplotype is a paradigm for non-Mendelian inheritance (Schimenti 2000; Lyon 2003). This variant of chromosome 17 is transmitted at excess rates (up to 99%) from *t/+* heterozygous males to their offspring (Chesley and Dunn 1936). This phenomenon, termed transmission ratio distortion (TRD), is caused by the action of several *t complex*

distorters (*Tcd1–4*), which additively enhance the transmission rate of the *t complex responder* (*Tcr*) (Lyon 1984). On the physiological level, TRD has been attributed to alteration of motility parameters in wild-type sperm derived from *t/+* males (Katz et al. 1979; Olds-Clarke and Johnson 1993).

Tcr (gene symbol *Smok1^{Tcr}*, herein abbreviated *Tcr*) was identified as a dominant-negative allele of the *sperm motility kinase-1* (*Smok1*) (Herrmann et al. 1999). This finding suggested that *Tcds* are involved in signaling pathways controlling sperm motility via *Smok1*. Indeed, molecular cloning of *Tcd1a* and *Tcd2* has identified regulators of Rho small G-proteins, *Tagap1* and *Fgd2*, linking TRD to Rho signaling pathways (Bauer et al. 2005, 2007).

The current model of TRD suggests that *Tcds* additively contribute to deregulation of two Rho signaling cascades that control wild-type *Smok1* protein (Bauer et al. 2005, 2007). The activating pathway is up-regulated, while the repressing pathway is down-regulated, by the *Tcd* gene products. The resulting hyperactivation of *Smok1* compromises the flagellar motility of all (*t* and +) sperm derived from a *t/+* male. The dominant-negative action of *Tcr* is able to specifically rescue *t* sperm from this “poisonous” effect of the *Tcds* via an unknown mechanism (Herrmann et al. 1999). Thus, *t/+* males produce two phenotypically distinct sperm populations, *t* sperm and + sperm, which differ in sperm motility, leading to an advantage of *t* sperm in fertilizing the egg cells (Supplemental Fig. 1).

This phenotypic difference between *t* sperm and + sperm contradicts the proposed phenotypic equivalence between gametes, enabled by sharing of gene products between meiotic partners (Braun et al. 1989; Ventela et al. 2003). The latter has been demonstrated with a reporter transgene expressed exclusively in post-meiotic germ cells in hemizygous males (Braun et al. 1989). More recent experiments demonstrated microtubuli-dependent active transport of ribonucleoprotein (RNP) particles between haploid spermatids (Ventela et al. 2003). Thus, the question remained as to how *Tcr* causes gametic inequality.

Results and Discussion

We asked whether *Tcr* was able to escape the mechanism of gene product sharing between germ cells. To answer this question, we isolated the *Tcr* promoter and constructed a *Tcr* minigene that included a Myc epitope tag at the N terminus of the *Tcr* ORF (Myc-*Tcr*) (Fig. 1A). The construct [*Tg(Smok*^{Tcr})9-987Bgh*, abbreviated *Tg9*] was introduced into the germline of mice. To ensure that this construct is able to cause TRD-like endogenous *Tcr*, we tested transgenic males for the transmission rate of *Tg9* in the presence of *Tcd* genes. *Tg9/0* males were crossed to females carrying the partial *t* haplotype *t^{h51}t^{h18}* comprising several of the *Tcd* loci, but not *Tcr* (Lyon 1984). Male offspring of the genotype *Tg9/0;t^{h51}t^{h18}/++* were crossed to wild-type females, and their litters were tested for the transmission rate of *Tg9*. We found that 76.6% of their offspring inherited the *Tg9* construct (Table 1). Deviation from the Mendelian ratio was highly significant, demonstrating that *Tg9* expresses *Tcr* function comparable with endogenous *Tcr* (Lyon 1984). On the

[**Keywords:** Mouse; *t* haplotype; non-Mendelian inheritance; transmission ratio distortion; spermatogenesis; motility]

⁶Present address: Hamilton Institute, National University of Ireland, Maynooth, County Kildare, Ireland

⁷Corresponding author.

E-MAIL herrmann@molgen.mpg.de; FAX 49-30-8413-1229.

Article is online at <http://www.genesdev.org/cgi/doi/10.1101/gad.553009>.

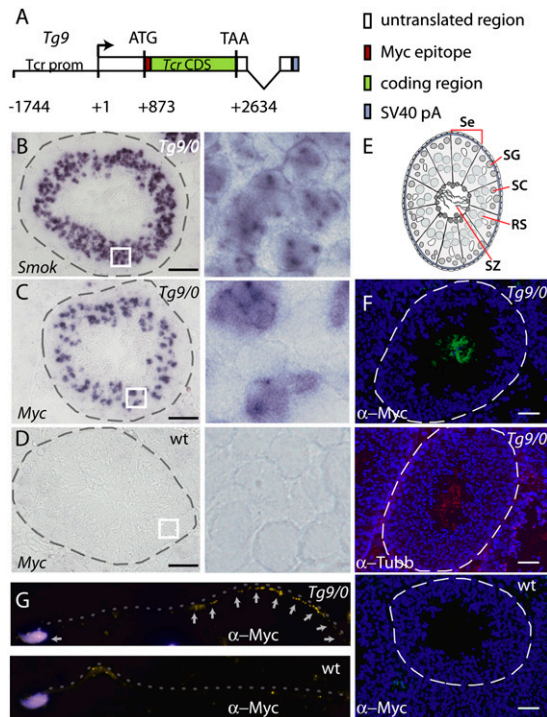


Figure 1. *Tcr* transcripts escape the general mechanism of product sharing between syncytial sperm cells and are translated at late stages of spermiogenesis. (A) Schematic drawing of the transgene construct *Tg9* comprising the *Tcr* promoter (*Tcr* prom), untranslated region, and Myc epitope-tagged *Tcr* coding region (*Tcr* CDS), followed by the simian virus polyadenylation signal (SV40pA). (B–D) Cryosections of *Tg9/0* (B,C) or wild-type (D) testes hybridized in situ with digoxigenin (DIG)-labeled *Smok1*-specific (B) or Myc epitope-specific (C,D) probes, showing expression of endogenous *Smok1* transcripts in all round spermatids (B), whereas *Tg9* transcripts are confined to a subpopulation of round spermatids (C) and not detected in the control (D). Dashed lines indicate the outlines of seminiferous tubules, and white boxes indicate subregions shown at higher magnification on the right. Bar, 100 μ m. (E) Schematic view of a seminiferous tubule. (Se) Sertoli cells; (SG) spermatogonia; (SC) spermatocytes; (RS) round spermatids; (SZ) spermatozoa. (F, top panel) Immunofluorescent detection of Myc-Tcr protein using an anti-Myc antibody (α -Myc) on testis cryosections of a *Tg9/0* male reveals Tcr protein in the lumen of seminiferous tubules. (Middle panel) β -Tubulin (α -Tubb), a major component of axonemes, indicating flagella, localizes to the same region. (G) In epididymal spermatozoa, Myc-Tcr localizes primarily to the principal piece and nucleus (yellow arrows; the flagellum is indicated by a dashed line). (F,G, bottom panel) Wild-type controls show some nonspecific primary antibody reaction. Nuclei are visualized by DAPI staining (blue). Bar, 50 μ m.

wild-type background, in the absence of *Tcd* activity, the transgene had no statistically significant effect.

RNA expression of the transgene construct was analyzed by in situ hybridization of cryosections derived from testes of adult hemizygous males (Fig. 1B,C). To distinguish *Tg9*-derived transcripts from endogenous *Smok1* expression, we used a probe specific for the Myc epitope tag of the transgene (Fig. 1C). Expression of wild-type *Smok1* was analyzed on consecutive sections hybridized with a *Smok1*-specific probe (Fig. 1B). Both probes produced signals in a broad ring of cells located between the outer basal lamina and the lumen of seminiferous tubules, representing haploid round spermatids (Russell et al. 1990). Thus, the *Tcr* promoter used for the *Tg9* construct

confers the same spatial and temporal expression pattern as the endogenous *Smok1* promoter, suggesting that it reflects the activity of the endogenous *Tcr* gene promoter (Herrmann et al. 1999). Our data showed that the RNA expression of *Smok1* and *Tcr* is confined to haploid spermatids (Fig. 1B,C,E; Supplemental Fig. 2).

Tcr expression from the *Tg9* transgene construct was analyzed in hemizygous males, and thus transcription of *Tg9* is expected to take place only in the cells that obtained the transgene during meiosis—approximately half of the haploid round spermatids (Braun et al. 1989). Yet, if the RNA products were distributed throughout the syncytium, the *Tg9*-derived transcripts should be detectable in all round spermatids. However, we detected *Tg9*-derived RNA in only approximately half of the round spermatids. Therefore, our data suggest that *Tcr* transcripts escape the general mechanism of gene product sharing between neighboring cells of the syncytium (Braun et al. 1989) and remain, perhaps tethered, in the cells of origin (Fig. 1C). Indeed, high-resolution imaging showed that *Smok1* as well as *Tg9*-derived *Tcr* transcripts occur mostly in RNA aggregates located inside or attached to the nucleus, consistent with retention of the RNA close to the site of production (Fig. 2).

RNA tethering, however, is not sufficient for haploid restriction of *Tcr* activity (Braun et al. 1989). Translational repression would also be required to prevent distribution of the protein between gametes. Therefore, we asked at what stage of spermatogenesis *Tcr* transcripts are translated. Testis sections derived from *Tg9/0* males were immunostained with anti-Myc antibody to visualize Myc-Tcr protein by immunofluorescence. We observed Myc-Tcr in only the luminal region of seminiferous tubules of testes derived from *Tg9* carrier males, but not in wild-type controls (Fig. 1F; Supplemental Fig. 3). The luminal aspect of seminiferous tubules harbors sperm cells reaching the end of differentiation as well as mature spermatozoa, which are released for transport to the epididymes (Russell et al. 1990). Much of the lumen is filled with flagella, as visualized by immunofluorescent detection of β -tubulin, a major component of the axoneme. High-resolution imaging of immunostained spermatozoa derived from the cauda epididymis revealed Myc-Tcr protein in the principal piece of flagella and in sperm nuclei (Fig. 1G). Thus, we conclude that Myc-Tcr protein is translated in flagellated spermatids and localized in the principal piece and nucleus of sperm.

The protein expression pattern of *Tcr* revealed an unexpected substantial delay between the onset of transcription in round spermatids and the appearance of protein in the flagella of late spermatids. These findings suggest high stability concomitant with strong translational repression of the *Tcr* transcripts throughout spermiogenesis. Although post-transcriptional control and translational repression are quite common for spermatogenic genes (Braun 1998; Hecht 1998), to our knowledge, such a late onset of protein expression during spermiogenesis has not yet been reported.

Immunofluorescent detection of Myc-Tcr on isolated spermatozoa did not allow for analysis of Tcr distribution, namely, if between meiotic partners or if retained in the cells of origin. To analyze this, we used high-resolution electron microscopy techniques to detect gold-labeled anti-Myc immunostaining of Myc-Tcr on ultrathin sections of spermatozoa contained in the epididymis of *Tg9/0* males.

Table 1. The transgene construct *Tg9* causes non-Mendelian inheritance in the presence of *Tcds*

Genotype of male	Number of males	<i>Tg</i>	Offspring				
			Non- <i>Tg</i>	Total	Percent <i>Tg</i>	χ^2	<i>P</i> -value
<i>Tg9/0; t^{h51}t^{h18}/++</i>	3	143	39	182	76.6%	59.4	1.27×10^{-14a}
<i>Tg9/0; ++/++</i>	3	141	113	254	55.5%	3.09	0.0789 ^b

χ^2 method was used.

^aSignificant non-Mendelian inheritance (*P*-value \ll 0.05).

^bNonsignificant deviation from Mendelian inheritance (*P*-value > 0.05).

Gold particles were detected in sperm nuclei and in flagella of epididymal spermatozoa (Fig. 3). Gold particles observed in the flagella localized to outer dense fibers (ODFs) and at the transversal ribs of the fibrous sheath (Fig. 3A), consistent with a putative role of *Tcr* in flagellar motility. These flagellar structures are known to anchor components of Rho signaling pathways (Fujita et al. 2000; Eddy et al. 2003), further supporting a functional link between *Tcr* and Rho signaling, as revealed previously by genetic data (Bauer et al. 2005, 2007). The significance of *Tcr* protein in the sperm nucleus remains unclear.

Immunogold particles were counted from 204 and 202 sections of sperm nuclei derived from the epididymis of *Tg9/0* and wild-type control males, respectively. In the control sample (wild type), about two-thirds of the sperm nuclei were devoid of immunogold particles; however, the remainder showed low counts of false-positive staining (up to four particles per sperm nucleus). In contrast, *Tg9/0*-derived sperm heads showed considerably higher gold particle counts (up to 22 particles) in two-thirds of the sections, whereas about one-third of the sections contained no particles at all (Fig. 3C). Statistical analysis revealed the nonhomogeneous distribution of particle counts in *Tg9/0*-derived sperm was due to a significant subpopulation of sperm being wild type with respect to *Myc-Tcr* protein. Maximum likelihood estimation indicated that this subpopulation amounts to about half of the sperm (Supplemental Material). Therefore, consistent with previous observations (Fig. 1C) we conclude that *Tcr* protein is retained in the haploid sperm cells expressing the gene.

Our data provide a plausible molecular explanation for phenotypic inequality of sperm derived from *t/+* males, leading to TRD. We show that *Tcr* is post-meiotically transcribed in haploid spermatids, and the mRNA is translationally repressed and tethered, preventing transport to neighboring cells. Delayed translation of the mRNA just prior to, or after, individualization of spermatozoa appears to prevent distribution of the protein between the gametes. Alternatively, translation of the mRNA may occur concomitant with the formation of flagella, and the *Tcr* protein might be specifically transported to the principal piece (Kierszenbaum 2002) and anchored at the fibrous sheath and ODFs.

This is strikingly in contrast to *Tcds*, as exemplified by *Tagap1* and *Fgd2*, which are expressed premeiotically in diploid spermatocytes (Bauer et al. 2005, 2007). Their gene products are expressed in all cells of the syncytium and compromise the flagellar function of all spermatozoa derived from a *t/+* male (Bauer et al. 2005, 2007). Due to haploid restriction of *Tcr* gene products, which have rescuing activity, only *t* sperm are rescued from the deleterious effect of the *Tcds*. Thus, + sperm remain

defective and *t* sperm gain an advantage in reaching and fertilizing egg cells. In that manner, it is apparent that *Tcr* takes advantage of the *Tcd* function and selfishly uses its special properties to promote its own transmission to the next generation. However, since the *Tcds* and *Tcr* are locked in a linkage group protected from splitting up by recombination suppression (Lyon 1984), the *Tcd* genes may also profit from the enhanced transmission rate of *Tcr*.

Since *Tcr* is a mutated gene, we questioned whether the tethering of transcripts and late translation of *Tcr* transcripts, which enables haploid restriction of *Tcr* function, are due to neomorphic mutations, and thus are unique to *Tcr* or, alternatively, exist also in wild-type *Smok1*, the progenitor of *Tcr*. If the latter were true, it would suggest that similar properties also exist in other genes not associated with *t* haplotype-dependent TRD, since it is

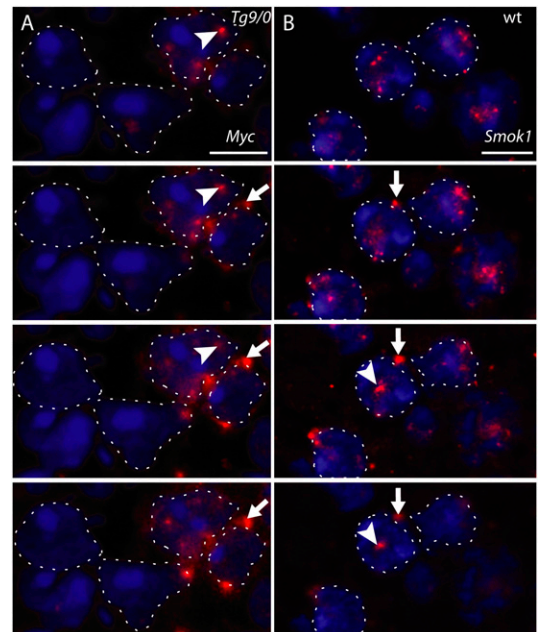


Figure 2. *Tcr* and *Smok1* transcripts occur mainly in nuclear and perinuclear aggregates. Serial optical sections ($\sim 1\text{-}\mu\text{m}$ depth) of testicular cryosections obtained by confocal microscopy visualizing *Tg9* (A) or *Smok1* (B) transcripts (red) detected by fluorescent in situ hybridization in round spermatids. Selected examples of nuclear (arrowhead) and perinuclear (arrow) RNA aggregates are indicated. *Tg9* transcripts were detected on sections of *Tg9/0*-derived testes (shown in A) with a DIG-labeled *Myc* epitope-specific probe, and *Smok1* transcripts were detected on sections of wild-type testes with a *Smok1*-specific probe. Dashed lines denote the nuclear outlines of round spermatids visualized by DAPI staining (blue), and bright blue structures within the nuclei represent nucleoli. Bar, 6.5 μm .

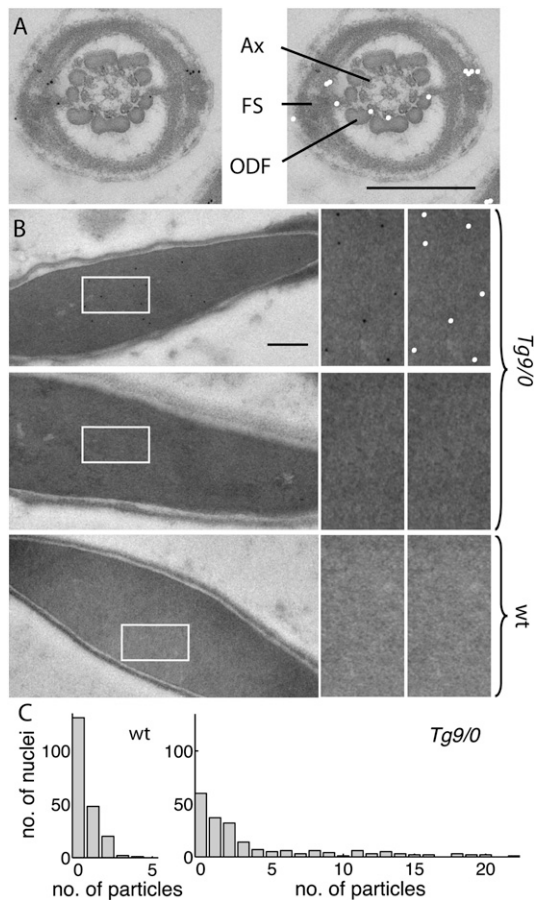


Figure 3. Tcr protein is retained in the spermatozoa expressing the transgene. (A,B) Ultrathin sections of spermatozoa derived from the cauda epididymis of *Tg9/0* or wild-type control (wt) males assayed for Myc-Tcr protein using immunogold-labeled anti-Myc antibodies reveals the localization of Tcr protein at the fibrous sheath (FS) and the ODFs of the principal piece of the flagellum (A) and in sperm nuclei (B). A fraction of *Tg9/0*-derived sperm nuclei show no or few immunogold particles, like wild-type sperm. White boxes indicate areas shown at higher magnification on the right; for better visualization, immunogold particles are shown as white spots on duplicate panels. (Ax) Axoneme. Bars: A, 500 nm; B, 280 nm. (C) Histograms showing the number of sections of sperm nuclei corresponding to the number of immunogold particles counted, based on the analysis of 202 and 204 sperm nuclei derived from wild-type (wt) or *Tg9/0* animals, respectively. In sperm nuclei of hemizygous *Tg9/0* males, one part of the distribution is concentrated at low immunogold particle counts, whereas the remainder is widely spread at higher counts (heavy tail distribution).

unlikely that such a refined mechanism of post-transcriptional regulation in haploid spermatids is unique to a single gene family. To answer this question, we investigated the properties of *Smok1* expressed from a transgene construct in hemizygous males. A minigene for wild-type *Smok1* (*TgS*) was constructed and introduced into the germline of mice (Fig. 4A). Males carrying *TgS* were tested for RNA and protein expression of the transgene construct, similar to *Tg9*. Our results show that the RNA and protein expression patterns of *TgS* are indistinguishable from those obtained with *Tg9*; i.e., restricted RNA expression in round haploid spermatids, tethering of the transcripts in the cells of origin, and late translation of the protein in flagellated spermatids (Fig. 4B,C).

These data suggest that the post-transcriptional control mechanisms revealed for *Tcr* and *Smok1* indeed existed prior to the evolution of *Tcr* from *Smok1*. Thus, this mechanism is most likely not rare in genes involved in sperm function, but simply has not been noticed before. It is conceivable that genes that are involved in sperm function, and whose products escape the sharing mechanism between spermatids (Martin-DeLeon et al. 2005), have the potential to evolve functionally different alleles, which may cause phenotypic inequality of gametes and non-Mendelian inheritance. We propose that the molecular mechanism regulating *Tcr/Smok1* elucidated here may be a common cause of non-Mendelian inheritance in mammals (Fig. 4D). It may also extend to humans, although it is unclear whether any of the non-Mendelian inheritance phenotypes described in humans thus far (Curtsinger et al. 1983; Van Heyningen and Yeyati 2004; Hesketh and Xing 2006; James 2009) relate to the mechanism shown here. Our data describing the regulation of *Tcr/Smok1* provide a molecular basis for the identification of other genes that may be involved in non-Mendelian inheritance. This will promote the

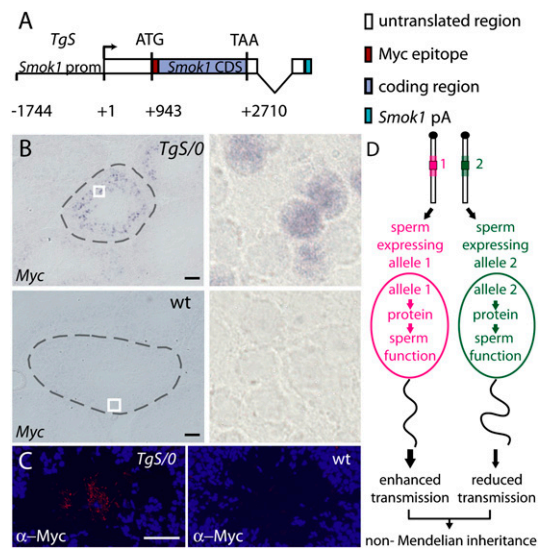


Figure 4. *Smok1* shows the same pattern of transcriptional expression and post-transcriptional control as *Tcr*. (A) Schematic drawing of the transgene construct *TgS*, consisting of the *Smok1* promoter (*Smok1* prom), the Myc epitope-tagged *Smok1* coding region (*Smok1* CDS), and untranslated regions followed by the polyadenylation signal (*Smok1* pA). (B) Testis cryosections of *TgS/0* (top panel) or wild-type control (bottom panel) males hybridized in situ with a DIG-labeled Myc epitope-specific probe (Myc) show *TgS* expression in seminiferous tubules of the *TgS/0* male in a subpopulation of round spermatids, but not in the control. White boxes indicate the regions shown at higher magnification on the right, and the borders of seminiferous tubules are indicated by dashed lines. Bar, 100 μ m. (C) Immunofluorescent detection of Myc-Smok1 protein on cryosections of seminiferous tubules derived from a *TgS/0* (left panel) or a wild-type control (right panel) male using anti-Myc antibodies visualizing Myc-Smok1 protein (red) specifically in the lumen filled with flagella of late-stage spermatids. Nuclei are visualized by DAPI staining (blue). Bar, 50 μ m. (D) Model depicting a mechanism leading to non-Mendelian inheritance of functionally different alleles (denoted 1 and 2), as well as genetically linked chromosomal regions (shaded area), of a gene involved in sperm function due to post-meiotic expression and retention of the gene products in the haploid spermatids, thus creating functionally different spermatozoa.

investigation of this striking phenomenon in humans and other organisms.

Materials and methods

Generation of transgenic mice

The *Tcr* transgene construct *Tg(Smok**Tcr*)9-987Bgh* (*Tg9*) consists of the *Tcr* promoter (1744 base pairs [bp] upstream of the transcriptional start site) and the *Tcr* 5'-untranslated region (UTR) amplified from testis cDNA, followed by six repeats (6×) of the Myc epitope fused N-terminally to the coding sequence of *Tcr*^{tw12}. The coding sequence and part of the 3'-UTR and intron 2 were obtained from *t*^{tw12} genomic DNA. In order to eliminate residual kinase activity of *Tcr*, we introduced the mutations D127A and D131A in subdomain VIb. To avoid the large *Rsk3*-derived 3'-UTR of *Tcr*, part of intron 2 and 141 bp of the third exon encoding 3'-untranslated sequences were derived from genomic DNA of *Smok1*^{tw12}. The remainder of the 3'-UTR and the polyadenylation signal of *Tg9* are derived from SV40 DNA.

For generation of the wild-type *Smok1* transgene *Tg(Smok1)1-8Bgh* (*TgS*), we amplified the *Smok1* promoter and the 5' end of the *Smok1* 5'-UTR from C57Bl/6J genomic DNA. To exclude intron 1 of the *Smok1* gene, we amplified the 3' end of the 5'-UTR sequence from testis cDNA (C57Bl/6J). The *Smok1* coding region, its 3'-UTR, intron 2, and polyadenylation signal were amplified from genomic DNA. The N terminus of the coding sequence was fused in-frame to a 6× Myc epitope tag, as for *Tg9*.

Transgenic constructs were isolated from the vector backbone and purified for pronuclear injection of fertilized C57Bl/6J eggs using standard procedures.

GenBank accession numbers are AJ245456 for *Tcr* AJ245452 and AJ245455 for *Smok1*^{C57BL/6}; *Smok*^{tw12}.

TRD tests

We backcrossed *Tg9* founders for at least four generations to the strain BTBR/TF +tf/+tf, our preferred strain for testing TRD (Gummere et al. 1986). We mated backcrossed *Tg9/0* animals to the partial *t* haplotype *t*^{h51,h18}/++ (BTBR/TF) carrying *Tcd1* and *Tcd2*, but not *Tcr* (Lyon 1984).

To determine the transmission rate of the *Tg9* transgene in the presence and absence of *Tcds*, we mated *Tg9/0;t*^{h51,h18}/++ (BTBR/TF) tester males and *Tg9/0;+/++* (BTBR/TF) control males with outbred females (NMRI). Embryos were dissected at 9–14 d post-coitum and lysed using standard procedures. After dilution of the lysate in water (1:20) and heat inactivation (20 min, 80°C), genotyping was performed by PCR using primers NV55 and NV34 (Supplemental Material).

To statistically analyze whether the transmission ratio of the transgene significantly deviates from the Mendelian ratio, we performed a χ^2 test (*Tg9/0;+/++*: $n = 254$, $\alpha = 0.05$; and *Tg9/0;t*^{h51,h18}/++: $n = 182$, $\alpha = 0.05$).

Transcript analysis

In situ hybridization was performed on 10- μ m testis cryostat sections essentially as described (Brent et al. 2003). We detected transgenic transcripts from *Tg9* and *TgS* using a digoxigenin (DIG)-labeled riboprobe hybridizing to the 6× Myc epitope tag. To generate the template for probe synthesis, we subcloned a PCR fragment (primers NV33 and NV34; Supplemental Material) containing the 6× Myc sequence amplified from *Tg9* into pCRII-TOPO (Invitrogen) and obtained riboprobes by antisense in vitro transcription from this vector. For the detection of endogenous wild-type *Smok1* transcripts, we PCR-amplified 1.3 kb of the protein-coding region of *Smok1* (129Sv) from a 2.2-kb genomic EcoRI fragment of the *Smok1* gene in pBS-KS (primers BGH170 and NV19; Supplemental Material). We subcloned the PCR fragment in pCRII-TOPO and used it as a template for in vitro transcription of a DIG-labeled antisense riboprobe. For the development of the fluorescent in situ hybridization signal, we used Fast Red Substrate (DAKO), as recommended by the supplier. Nuclei were counterstained with DAPI.

Immunofluorescence detection of protein on testis sections and epididymal sperm

We performed immunofluorescence detection of protein on testis cryostat sections after pretreatment of the tissue as described (Brent et al. 2003).

Testis sections of *Tg9/0* and BTBR/TF control animals were blocked with PBS, 0.2% Tween (PBS-T) and 5% normal goat serum (Vector Laboratories), and incubated with a mouse monoclonal anti-Myc antibody (1:100; clone 4A6, Upstate Biotechnologies) or a rabbit polyclonal anti-Myc antibody (1:100; Sigma, C3956) and, subsequently, with a peroxidase-coupled sheep anti-mouse or a donkey anti-rabbit IgG (both from Amer-sham Biosciences), respectively. Signals were amplified by FITC-coupled TSA (Perkin Elmer) substrate reaction as recommended by the supplier. For β -tubulin staining on *Tg9/0* testis sections, we used a mouse monoclonal anti- β -tubulin antibody from ascites fluid (1:100; Sigma, T5293) and a Cy3-coupled goat anti-mouse IgG (Jackson ImmunoResearch).

Immunofluorescence on testis sections of transgenic *TgS/0* and BTBR/TF control animals was performed by blocking with PBS-T and 5% normal goat serum, and incubation with a mouse monoclonal anti-Myc antibody (1:100; clone 4A6, Upstate Biotechnologies) and, subsequently, with a Cy3-coupled goat anti-mouse IgG. Nuclei were counterstained with DAPI.

For the visualization of *Tcr* protein in sperm, mature spermatozoa were isolated from the cauda epididymis and pretreated as described (Braun et al. 1989). Briefly, sperm was capacitated, washed, spread on glass slides, and fixed with 4% PFA/PBS. After a blocking step with 5% normal goat serum in PBS-T, we incubated fixed spermatozoa with a rabbit polyclonal anti-Myc antibody (1:100; Sigma C3956) and Qdot 655-conjugated goat anti-rabbit IgG (Invitrogen). Sperm nuclei were counterstained with DAPI. Qdot 655 fluorescence was monitored using a suitable filter set (Chroma Technology).

Electron microscopy of sperm

Cauda epididymis containing mature spermatozoa was isolated from *Tg9/0* males and from BTBR/TF control animals, dissected in fixative (glutaraldehyde, PFA), and fixed overnight at 4°C. Tissues were dehydrated in an ethanol series, transferred to LR white resin (Electron Microscopy Sciences), polymerized for 72 h at 42°C, and subsequently cut into 70-nm ultrathin sections. Immunogold labeling was performed with a rabbit polyclonal anti-Myc antibody (Sigma) and 10 nm of gold-conjugated anti-rabbit IgG (British Biocell) and documented by electron microscopy on a CCD-camera (FastScan, TVIPS).

Sperm nuclei areas and respective gold particle counts were subsequently analyzed on digital pictures (ImageJ software) and statistically analyzed as described below.

Statistical analysis of immunogold particle counts

To analyze the distribution of *Tcr* protein among sperm from *Tg9/0* hemizygous mice, we assumed that the particle counts obtained from immunogold labeling are Poisson distributed, which follows if binding events occur independently of each other with a constant rate (Gardiner 2004; Ewens and Grant 2005). Using sperm from wild-type mice, we studied the false-positive signal caused by the labeling technique. Based on this estimate, and considering the number of sperm that showed no particles, we carried out a binomial test ($n = 51$, $\alpha = 0.01$) to analyze whether, in *Tg9/0*-derived sperm, *Tcr* is distributed to all sperm or whether it remains restricted to a subpopulation of sperm, and applied maximum likelihood estimation to estimate the proportion of the subpopulation devoid of *Tcr* protein (Supplemental Material).

Acknowledgments

We thank Rudi Lurz for electron microscopy, M.F. Lyon for mice carrying the *t* haplotypes used in this study, Vijay Subramanian for suggestions and discussions about statistical approaches, Ingo Voigt for pronuclear injection, Ludger Hartmann for supervision of the animal facility, Carolin Willke for expert animal caretaking, and Alexandra Farrall and Phillip Grote for critical comments on the manuscript. This project was supported by a grant from the Deutsche Forschungsgemeinschaft to B.G.H.

References

Bauer H, Willert J, Koschorz B, Herrmann BG. 2005. The *t* complex-encoded GTPase-activating protein tagap1 acts as a transmission ratio distorter in mice. *Nat Genet* 37: 969–973.

- Bauer H, Veron N, Willert J, Herrmann BG. 2007. The t-complex-encoded guanine nucleotide exchange factor Fgd2 reveals that two opposing signaling pathways promote transmission ratio distortion in the mouse. *Genes & Dev* **21**: 143–147.
- Braun RE. 1998. Post-transcriptional control of gene expression during spermatogenesis. *Semin Cell Dev Biol* **9**: 483–489.
- Braun RE, Behringer RR, Peschon JJ, Brinster RL, Palmiter RD. 1989. Genetically haploid spermatids are phenotypically diploid. *Nature* **337**: 373–376.
- Brent AE, Schweitzer R, Tabin CJ. 2003. A somitic compartment of tendon progenitors. *Cell* **113**: 235–248.
- Chesley P, Dunn LC. 1936. The inheritance of taillessness (anury) in the house mouse. *Genetics* **21**: 525–536.
- Curtsinger J, Ito R, Hiraizumi Y, Curtsinger JW. 1983. A two-generation study of human sex-ratio variation. *Am J Hum Genet* **35**: 951–961.
- Eddy EM, Toshimori K, O'Brien DA. 2003. Fibrous sheath of mammalian spermatozoa. *Microsc Res Tech* **61**: 103–115.
- Ewens WJ, Grant G. 2005. *Statistical methods in bioinformatics*. Springer, New York.
- Fujita A, Nakamura K, Kato T, Watanabe N, Ishizaki T, Kimura K, Mizoguchi A, Narumiya S. 2000. Ropporin, a sperm-specific binding protein of rhophilin, that is localized in the fibrous sheath of sperm flagella. *J Cell Sci* **113**: 103–112.
- Gardiner CW. 2004. *Handbook of stochastic methods: For physics, chemistry and the natural sciences*. Springer, New York.
- Gummere G, McCormick P, Bennett D. 1986. The influence of genetic background and the homologous chromosome 17 on t-haplotype transmission ratio distortion in mice. *Genetics* **114**: 235–245.
- Hecht NB. 1998. Molecular mechanisms of male germ cell differentiation. *Bioessays* **20**: 555–561.
- Herrmann B, Koschorz B, Wertz K, McLaughlin K, Kispert A. 1999. A protein kinase encoded by the t complex responder gene causes non-mendelian inheritance. *Nature* **402**: 141–146.
- Hesketh T, Xing ZW. 2006. Abnormal sex ratios in human populations: Causes and consequences. *Proc Natl Acad Sci* **103**: 13271–13275.
- Hurst GD, Werren JH. 2001. The role of selfish genetic elements in eukaryotic evolution. *Nat Rev Genet* **2**: 597–606.
- James WH. 2009. The variations of human sex ratio at birth during and after wars, and their potential explanations. *J Theor Biol* **257**: 116–123.
- Katz D, Erickson R, Nathanson M. 1979. Beat frequency is bimodally distributed in spermatozoa from t/t12 mice. *J Exp Zool* **210**: 529–535.
- Kierszenbaum AL. 2002. Intramanchette transport (imt): Managing the making of the spermatid head, centrosome, and tail. *Mol Reprod Dev* **63**: 1–4.
- Lyon MF. 1984. Transmission ratio distortion in mouse t-haplotypes is due to multiple distorter genes acting on a responder locus. *Cell* **37**: 621–628.
- Lyon MF. 2003. Transmission ratio distortion in mice. *Annu Rev Genet* **37**: 393–408.
- Martin-DeLeon PA, Zhang H, Morales CR, Zhao Y, Rulon M, Barnoski BL, Chen H, Galileo DS. 2005. Spaml-associated transmission ratio distortion in mice: Elucidating the mechanism. *Reprod Biol Endocrinol* **3**: 32. doi: 10.1186/1477-7827-3-32.
- Olds-Clarke P, Johnson LR. 1993. T haplotypes in the mouse compromise sperm flagellar function. *Dev Biol* **155**: 14–25.
- Russell L, Ettlin R, Hikim A, Clegg E. 1990. *Histological and histopathological evaluation of the testis*. Cache River Press, Saint Louis, MO.
- Schimmenti J. 2000. Segregation distortion of mouse t haplotypes the molecular basis emerges. *Trends Genet* **16**: 240–243.
- Van Heyningen V, Yeyati PL. 2004. Mechanisms of non-Mendelian inheritance in genetic disease. *Hum Mol Genet* **13**: R225–R233. doi: 10.1093/hmg/ddh254.
- Ventela S, Toppari J, Parvinen M. 2003. Intercellular organelle traffic through cytoplasmic bridges in early spermatids of the rat: Mechanisms of haploid gene product sharing. *Mol Biol Cell* **14**: 2768–2780.